Multiple Antibiotic Resistance in Arabidopsis Is Conferred by Mutations in a Chloroplast-Localized Transport Protein[C][W][OA]

Sarah Conte*, David Stevenson, Ian Furner, and Alan Lloyd

Section of Molecular Cell and Developmental Biology, Institute for Cellular and Molecular Biology, University of Texas, Austin, Texas 78712 (S.C., A.L.); and Department of Genetics, Cambridge University, Cambridge CB2 3EH, United Kingdom (D.S., I.F.)

Widespread antibiotic resistance is a major public health concern, and plants represent an emerging antibiotic exposure route. Recent studies indicate that crop plants fertilized with antibiotic-laden animal manure accumulate antibiotics; however, the molecular mechanisms of antibiotic entry and subcellular partitioning within plant cells remain unknown. Here, we report that mutations in the Arabidopsis (*Arabidopsis thaliana*) locus *Multiple Antibiotic Resistance1* (*MAR1*) confer resistance, while *MAR1* overexpression causes hypersensitivity to multiple aminoglycoside antibiotics. Additionally, yeast expressing *MAR1* are hypersensitive to the aminoglycoside G418. *MAR1* encodes a protein with 11 putative transmembrane domains with low similarity to ferroportin1 from *Danio rerio*. A MAR1:yellow fluorescent protein fusion localizes to the chloroplast, and chloroplasts from plants overexpressing *MAR1* accumulate more of the aminoglycoside gentamicin, while *mar1-1* mutant chloroplasts accumulate less than the wild type. *MAR1* overexpression lines are slightly chlorotic, and chlorosis is rescued by exogenous iron. *MAR1* expression is also down-regulated by low iron. These data suggest that MAR1 is a plastid transporter that is likely to be involved in cellular iron homeostasis and allows opportunistic entry of multiple antibiotics into the chloroplast.

The amount of antibiotics used nontherapeutically in agriculture is estimated to be 8 times greater than the amount used in all of human medicine (Mellon et al., 2001) and accounts for about 70% of total antibiotic use in the United States (Florini et al., 2005). It is also estimated that approximately 75% of antibiotics are not absorbed in the gut and are excreted largely unchanged (Mackie et al., 2006; Sarmah et al., 2006). Many of these antibiotics retain activity in soil for long periods of time (Chander et al., 2005). Agricultural crops are routinely fertilized with livestock waste, which has led to widespread antibiotic contamination of the environment and contributed to the selection of resistant bacteria, threatening human health. Two obvious reservoirs of residual antibiotics in the environment are farm soil and groundwater, and recent studies have shown that crop plants accumulate antibiotics after growth on antibiotic-contaminated soils (Kumar et al., 2005; Boxall et al., 2006). This poses a public health concern, as continual, low-level exposure to antibiotics through produce consumption may foster the development of resistant bacteria (Hocquet et al., 2003). Despite concerns, virtually nothing is known about how plants are capable of taking up and distributing antibiotics, both within the plant body and on a subcellular level.

Endogenous mechanisms of antibiotic resistance in plants have not been well studied. Multiple drug resistance in bacteria is often conferred by multidrug efflux transporters encompassing several families, including (but not limited to) the ATP-binding cassette transporters, the major facilitator superfamily, and the multidrug and toxic compounds efflux family (Paulsen, 2003). There are only a few reports of antibiotic resistance in plants that are not based on expression of prokaryotic resistance genes, and three recent reports involve transporters. Overexpression of *AtWBC19*, from Arabidopsis (*Arabidopsis thaliana*), confers resistance to kanamycin in plants (Mentewab and Stewart, 2005). Our lab has found that overexpression of the Arabidopsis *multidrug resistance1* confers resistance to multiple herbicides and a single antibiotic, cycloheximide (Thomas et al., 2000; Windsor et al., 2003). The most recent report reveals that mutations in and RNA interference-based down-regulation of the putative transporter gene *RTS3* (for RNA-mediated Transcriptional gene Silencing) confer resistance to kanamycin (Aufsatz et al., 2009).

The sensitivity of plants to antibiotics that target prokaryotic translational machinery, such as spectino-

* Corresponding author; e-mail conte@mail.utexas.edu.

The author responsible for distribution of materials integral to the findings presented in this article in accordance with the policy described in the Instructions for Authors (www.plantphysiol.org) is: Alan Lloyd (lloyd@uts.cc.utexas.edu).

[C] Some figures in this article are displayed in color online but in black and white in the print edition.

[W] The online version of this article contains Web-only data.

[OA] Open access articles can be viewed online without a subscription.

www.plantphysiol.org/cgi/doi/10.1104/pp.109.143487

mycin, tetracycline, lincomycin, and the aminoglycosides, is attributed to the similarity of chloroplast ribosomes to bacterial ribosomes (Ellis, 1970; Kasai et al., 2004). In fact, it has been shown that mutations in chloroplast ribosomal subunits can confer resistance to various aminoglycosides (Kavanagh et al., 1994; Rosellini et al., 2004). This indicates that these antibiotics must not only enter the cell, but must also gain entry to the chloroplast in order to function—a process that requires passage across the plasma membrane as well as the chloroplast double membrane. Movement across membranes can be difficult for hydrophilic antibiotics, such as the aminoglycosides (Scholar and Pratt, 2000), and therefore may be facilitated by membrane transport proteins. Interestingly, the RTS3 putative transport protein is predicted to be chloroplast localized, indicating that it may be acting as an entry point for antibiotics into this subcellular compartment. However, no experimental evidence has yet been provided to support this prediction (Aufsatz et al., 2009). We have isolated three independent *rts3* mutants that also confer resistance to kanamycin, and we have found that this resistance extends to other aminoglycoside antibiotics as well. Additionally, we have expanded on the work of Aufsatz et al. to show chloroplast localization and transport functionality of RTS3.

Here, we refer to *RTS3* as *Multiple Antibiotic Resistance1* (*MAR1*). Both a single nucleotide change (*mar1-1*) and two independent T-DNA insertions (*mar1-2* and *mar1-3*) are able to confer resistance, which is highly specific to aminoglycosides that affect prokaryotic translational machinery. This resistance does not extend to antibiotics of other classes or to aminoglycosides that affect eukaryotic translational machinery. MAR1 is most likely a chloroplast envelope protein and appears to be a means by which antibiotics are able to opportunistically access their intracellular targets in a plant system. While the natural function of *MAR1* remains unknown, our preliminary experiments indicate that it may play a role in cellular iron homeostasis.

RESULTS

Isolation and Map-Based Cloning of the Multiple Antibiotic Resistant Mutant *mar1-1*

mar1-1 was generated via ethyl methanesulfonate (EMS) mutagenesis and was found to be resistant to several aminoglycoside antibiotics, including kanamycin, streptomycin, gentamicin, amikacin, tobramycin, and apramycin (Fig. 1, A and B). Interestingly, *mar1-1* was not found to be resistant to the aminoglycosides hygromycin, G418, or paromomycin (Supplemental Figs. S1 and S2). These compounds, while structurally similar to other aminoglycosides, are distinct in that they inhibit both prokaryotic and eukaryotic protein synthesis (Eustice and Wilhelm, 1984). No resistance was found to antibiotics of other classes, including spectinomycin (an aminocyclitol), tetracycline, chloramphenicol, and lincomycin (Fig. 1D). Each of these antibiotics target prokaryotic translational machinery but are structurally distinct from the aminoglycosides.

A backcross of *mar1-1* to the wild type revealed that the mutation is nuclear and monogenic. The mutant locus was isolated via map-based cloning. A single nucleotide change (C to T) was found in the 10th exon of the locus At5g26820 (Fig. 2A), which is annotated as having low similarity to *ferroportin1* from *Danio rerio*. At5g26820 has been described as *AtIREG3* based on sequence similarity to *AtIREG1* and *AtIREG2*, two iron-regulated transporters in Arabidopsis (Schaaf et al., 2006). More recently, it has been described as *RTS3*, and two mutations in the gene (*rts3-1* and *rts3-2*; Fig. 2, A and B) were shown to confer kanamycin resistance at 40 mg/L (Aufsatz et al., 2009).

Native expression of At5g26820 was able to complement the mutant *mar1-1* (data not shown). Here, we will refer to At5g26820 as *MAR1* since the gene name *RTS3* does not accurately describe the functionalities we have uncovered for At5g26820. The single nucleotide change in *mar1-1* leads to a single amino acid change (Ala to Val) at position 441 in the protein (A441V; Fig. 2B). This particular Ala residue lies in the middle of a putative transmembrane domain of the protein and is highly conserved among MAR1 homologs (Fig. 2C).

As mentioned earlier, *MAR1* has only two homologs in Arabidopsis, *AtIREG1* (At2g38460) and *AtIREG2* (At5g03570). However, there are three *MAR1* homologs in rice (*Oryza sativa*; Os12g3570, Os05g04120, and Os06g36450) and two homologs in grape (*Vitis vinifera*; A5AS54 and A5BT51). *MAR1* is more closely related to rice homologs that are predicted to be chloroplast localized (Os12g37530 and Os05g04120) and to its grape homolog that is predicted to function in secretory pathways (A5AS54; Fig. 2D; Schwacke et al., 2003). This could indicate that the MAR1 protein may localize to an intracellular compartment, as opposed to the plasma membrane of the cell.

The T-DNA Insertion Mutants *mar1-2* and *mar1-3* Phenocopy *mar1-1*

We obtained two T-DNA insertion lines for *MAR1* (Salk_034189 and Salk_009286) from the Arabidopsis Biological Resource Center. We have designated Salk_034189 as *mar1-2* and Salk_009286 as *mar1-3*. Both lines show an extreme reduction in MAR1 transcript, as measured by quantitative real-time PCR (Supplemental Fig. S3A), and both were found to be nearly phenotypically identical to *mar1-1*, with respect to antibiotic resistance (Fig. 1, A and C). Note that Salk lines are expected to be kanamycin and paromomycin resistant due to expression of *nptII*, but this does not lead to cross-resistance to other antibiotics, as illustrated by an unrelated kanamycin-resistant, *nptII*-

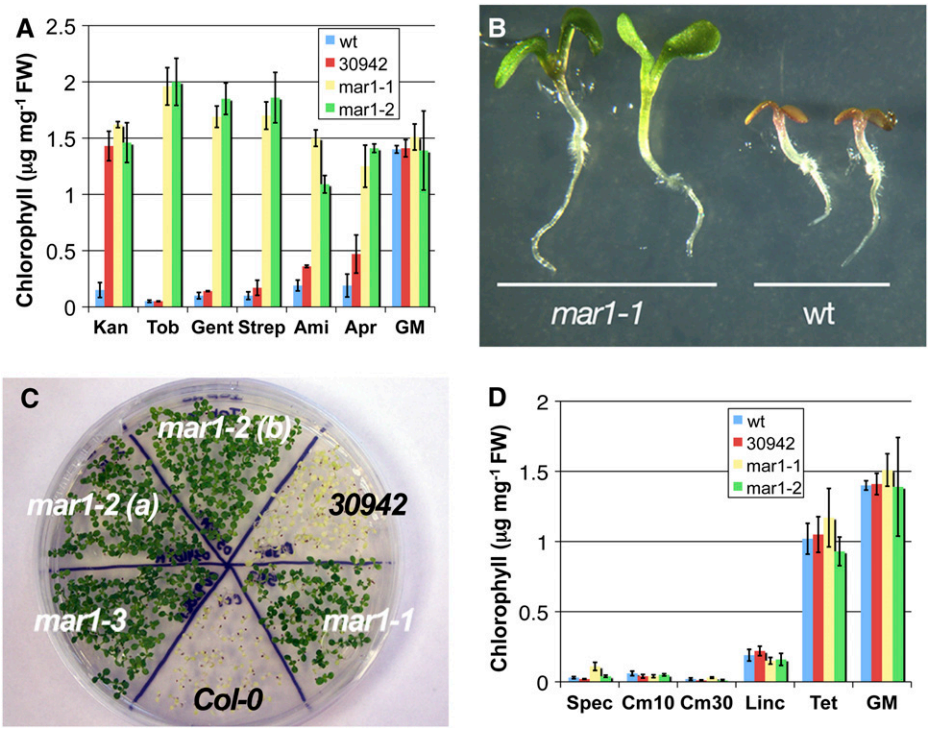

Figure 1. Resistance phenotypes of *mar1-1*, *mar1-2*, and *mar1-3*. A, Chlorophyll content of seedlings grown on aminoglycoside antibiotics. Wild-type (wt) seedlings and an unrelated homozygous T-DNA line, Salk_030942 (30942), were used as controls. Antibiotic concentrations were as follows: 25 mg/L kanamycin (Kan), 40 mg/L tobramycin (Tob), 70 mg/L gentamicin (Gent), 75 mg/L streptomycin (Strep), 100 mg/L amikacin (Ami), and 200 mg/L apramycin (Apr). GM was plain growth media (no antibiotic). B, Phenotypes of seedlings grown on MS media + kanamycin (25 mg/L) for 7 d. C, Phenotypes of the Salk T-DNA knockout mutants *mar1-2* [two individual homozygotes are indicated as (a) and (b)] and *mar1-3*, along with control line (30942) and Col-0, grown on MS media + tobramycin (40 mg/L) for 14 d. D, Chlorophyll content of seedlings grown as in A on media containing four non-aminoglycoside antibiotics. Antibiotic concentrations were as follows: 8 mg/L spectinomycin (Spec), 10 and 30 mg/L chloramphenicol (Cm10 and Cm30, respectively), 25 mg/L lincomycin (Linc), and 10 mg/L tetracycline (Tet). GM was plain growth media (no antibiotic). FW, Fresh weight. [See online article for color version of this figure.]

expressing Salk insertion line (Salk_030942; Fig. 1, A and C).

Overexpression of *MAR1* Confers Multiple Antibiotic Hypersensitivity

Since the T-DNA insertion lines *mar1-2* and *mar1-3* phenocopy the EMS mutant *mar1-1*, and all mutations confer multiple antibiotic resistance, we hypothesized that overexpressing *MAR1* would lead to the opposite phenotype: hypersensitivity to multiple antibiotics. We expressed the *MAR1* genomic locus from start to stop codon under control of the 35S promoter of *Cauliflower mosaic virus* in wild-type plants and found that it did confer a phenotype of hypersensitivity to both kanamycin and gentamicin, based on severe chlorosis and stunted growth of seedlings (Fig. 3, A and B). *MAR1* expression in two independent 35S overexpression lines was found to be at least 48-fold higher than the wild type (Supplemental Fig. S3B).

To further confirm that mutations in At5g26820 are responsible for the phenotype of *mar1*, we expressed 35S::At5g26820(*MAR1*) in the *mar1-1* background. Analysis of several independent transgenic lines revealed that this construct led to a reversal of the kanamycin resistance phenotype of *mar1-1*, i.e. mutant *mar1-1* plants overexpressing *MAR1* were found to be hypersensitive to kanamycin (Fig. 3C). Additionally, native expression of *MAR1* in a *mar1-2* background reverted the phenotype back to approximately wild-type levels of resistance (data not shown).

MAR1 Localizes to the Chloroplast Envelope

The ARAMEMNON plant membrane protein database (Schwacke et al., 2003) uses data from 17 individual programs to arrive at a consensus prediction for subcellular location. This consensus prediction method (Schwacke et al., 2007) predicts that the MAR1 protein is targeted to the chloroplast. According to the ChloroP program (Emanuelsson et al., 1999), the predicted chloroplast transit peptide of MAR1 includes the first 54 amino acids of the protein (Fig. 2B). A C-terminal yellow fluorescent protein (YFP)

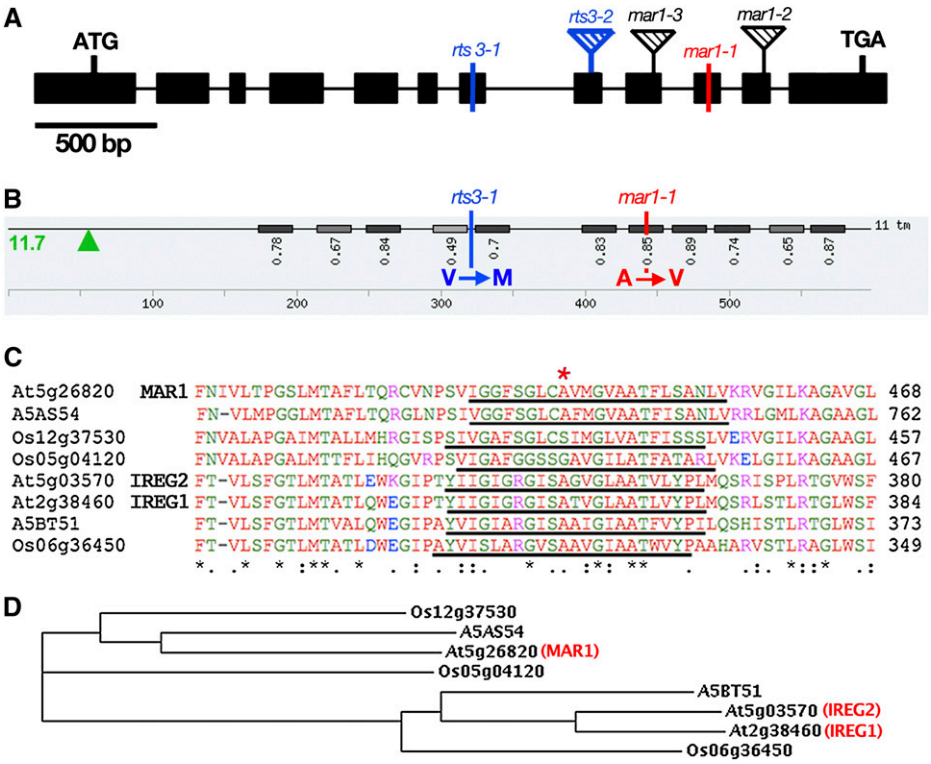

Figure 2. Analysis of the *MAR1* gene and protein. A, The *MAR1* gene in Arabidopsis. Exons are depicted as solid black boxes. The mutation sites for *mar1-1*, *rts3-1*, as well as insertion sites for SALK lines *mar1-2*, *mar1-3*, and GABI-KAT line *rts3-2* (Aufsatz et al., 2009) are shown. B, The MAR1 protein. Transmembrane domains in MAR1 are shown along with consensus score values (Schwacke et al., 2003). Domains with consensus scores above 0.42 are counted in the total number of transmembrane domains. A putative chloroplast transit peptide is predicted (with 11.7 consensus score value; Schwacke et al., 2003, 2007). The chloroplast transit peptide cleavage site (as predicted by ChloroP) is indicated with a green arrowhead. The amino acid changes in mutant *mar1-1* and *rts3-1* are also shown. C, Alignment of MAR1 (At5g26820) with its homologs in Arabidopsis (IREG2, At5g03570; IREG1, At2g38460), *O. sativa* (Os12g37530, Os05g04120, and Os06g36450), and *V. vinifera* (A5AS54 and A5BT51). Degree of conservation of various amino acids is indicated below the alignment by periods (highly conserved), colons (very highly conserved), and asterisks (completely conserved). Underlined areas illustrate the predicted transmembrane domains around the mutation site (as calculated by TMHMM, http://www.cbs.dtu.dk/services/TMHMM-2.0/). A red asterisk above the alignment indicates the site of the *mar1-1* mutation. D, Phylogram of MAR1 and related proteins listed in C. The alignment in C and phylogenetic tree in D were created using ClustalW (Larkin et al., 2007). [See online article for color version of this figure.]

fusion to the putative transit peptide of MAR1 was transiently expressed in Arabidopsis protoplasts. Chloroplast transit peptides are known to effectively mediate transport across the chloroplast membrane (Inaba and Schnell, 2008) so the expected localization of YFP fused to a transit peptide would be the stroma. This is what was observed in our experiment, based on distinct YFP colocalization with red (autofluorescent) chloroplasts (Fig. 4, F–H).

C-terminal and N-terminal translational fusions between full-length *MAR1* cDNA and YFP were also expressed. In C-terminal fusions, YFP fluorescence was clearly associated with chloroplasts (Fig. 4, J–L), and in N-terminal fusions, fluorescence was cytoplasmic (Fig. 4, O and P).

The MAR1-YFP C-terminal translational fusion described above was also used to transform plants. Expression of this fusion protein was able to complement the resistance phenotype of *mar1-2* (data not shown). Leaves of these plants were examined by confocal microscopy (Fig. 5, A–L) and compared to untransformed controls (Fig. 5, M–O). YFP fluorescence in transformed lines colocalized with chloroplast autofluorescence (Fig. 5, C, F, I, and L) and appeared particularly enhanced at the periphery of these organelles, indicating that MAR1 may be associated with the chloroplast envelope.

Expression of *MAR1* in Yeast Confers Hypersensitivity to the Aminoglycoside G418

To further test the function of the MAR1 putative transport protein, we expressed this protein in the yeast strain BY4700 under control of the strong PGK promoter. Both wild-type and *mar1-1* mutant alleles were used for these experiments. BY4700 was used because it is only slightly sensitive to the aminoglycoside G418 (authors' observations). Yeast expressing

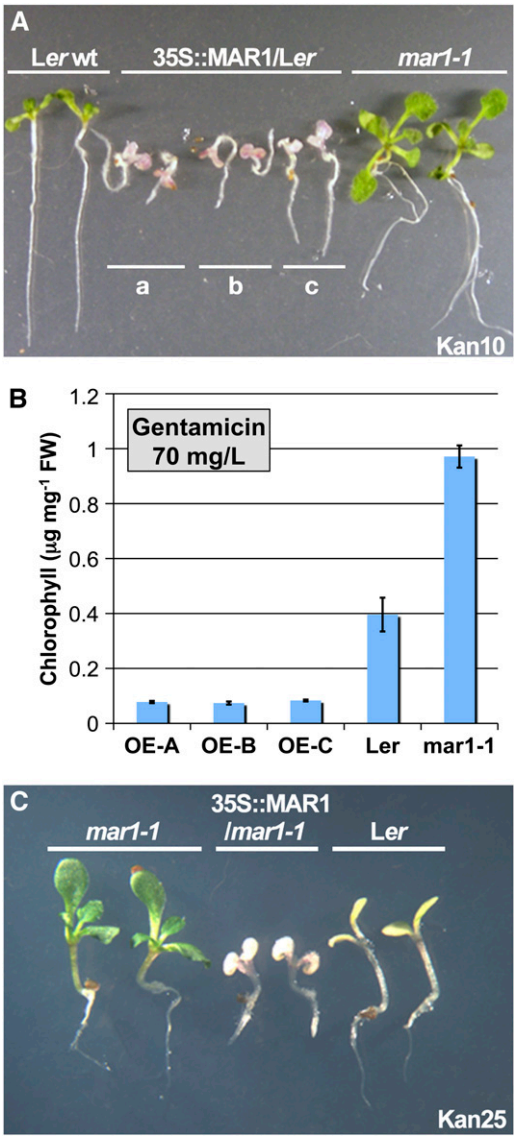

Figure 3. *MAR1* overexpression results in hypersensitivity to antibiotics. A, Seeds were plated on kanamycin (10 mg/L; Kan10). After 14 d, two representative seedlings of each line were photographed. Phenotypes of three independent overexpression lines are shown (a, b, and c). All lines are in the L*er* background. L*er* wt, L*er* wild type. B, Chlorophyll content (μg of chlorophyll per mg fresh weight [FW]) of *MAR1* overexpression lines grown for 2 weeks on media containing gentamicin (70 mg/L). OE-A, OE-B, and OE-C are three independent *MAR1* overexpression lines. Measurements represent the average chlorophyll content (±SD) of three separate batches of seedlings. C, Overexpression of *MAR1* in *mar1-1* background reverses the kanamycin resistance phenotype of *mar1-1*. Mutant *mar1-1* plants were transformed with 35S::*MAR1*, and seeds were plated on kanamycin (25 mg/L). After 14 d of growth, two representative seedlings were photographed. [See online article for color version of this figure.]

wild-type *MAR1* were found to be hypersensitive to G418 when compared to empty vector controls (Fig. 6A). Interestingly, yeast expressing the mutant allele *mar1-1* were also hypersensitive, but to a lesser extent than the *MAR1* yeast (Fig. 6A). To eliminate the possibility that hypersensitivity was due to a general toxicity effect, the experiment was repeated using varying concentrations of cycloheximide, which is highly toxic to yeast. No growth differences were seen, at any cycloheximide concentration, among yeast expressing either *MAR1*, *mar1-1*, or empty vector controls (Fig. 6B).

To ensure that MAR1 protein was being properly expressed, and to determine its localization pattern in yeast, we also expressed a GFP-tagged version of *MAR1*. Yeast expressing *MAR1-GFP* were hypersensitive to G418, indicating functionality of the fusion protein (data not shown). While GFP alone was clearly cytoplasmic (Fig. 6D), GFP-tagged MAR1 localized to the yeast mitochondria (Fig. 6C), which is typical for chloroplast membrane proteins expressed in yeast (Versaw and Harrison, 2002; Jeong et al., 2008). Since the aminoglycoside G418 acts on both prokaryotic and eukaryotic ribosomes (Vicens and Westhof, 2003), G418 is likely to be inhibiting yeast growth in *MAR1*-expressing strains by accumulating in mitochondria.

Since MAR1 was found to localize to the yeast mitochondria, we did an additional control using chloramphenicol, which is known to inhibit yeast mitochondrial translation (Ibrahim et al., 1974). We did not find resistance to chloramphenicol in *mar1-1* or *mar1-2* mutant plants (Fig. 1D); therefore, it is not likely to be a substrate for the MAR1 transporter. In support of this, we did not observe major growth differences between yeast lines expressing *MAR1* (or *mar1-1*) and empty vector controls when grown for 48 h in the presence of 0.5, 1, or 2 mg/mL chloramphenicol (Supplemental Fig. S4).

MAR1 Regulates Gentamicin Entry into Chloroplasts

Since MAR1 appeared to be a chloroplast-localized transport protein, and its disruption and overexpression caused antibiotic resistance and hypersensitivity, respectively, we decided to test its functionality as a transporter for antibiotics. To accomplish this, we developed both a short-term uptake assay using isolated chloroplasts and a longer-term uptake assay using whole seedlings. For short-term uptake, isolated chloroplasts were exposed to high levels of antibiotic (12.5 mg/mL) for short periods of time (1 and 5 min; Fig. 7A). For longer-term uptake, whole seedlings were exposed to lower levels of antibiotic (70 mg/L) for 2 d (Fig. 7D). Excess antibiotic was washed away, and chloroplasts were lysed to release their antibiotic content. Lysates were then spotted onto nitrocellulose in dot-blot fashion (Fig. 7C) along with gentamicin standards (Fig. 7B), and gentamicin was detected via anti-gentamicin antibody. This allowed for a simple yet quantitative method for measuring the gentamicin content of chloroplasts; each dot was analyzed using the integrated density function of ImageJ64 to determine a relative intensity value, which correlated positively with the amount of antibiotic in the lysate.

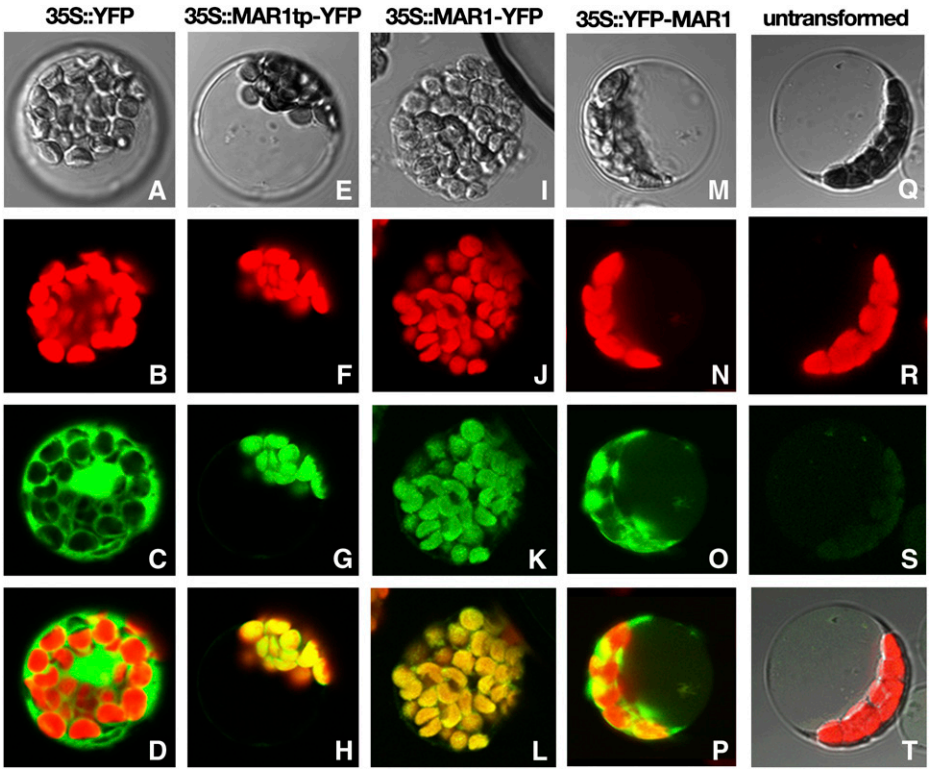

Figure 4. MAR1-YFP localizes to chloroplasts in protoplasts. Confocal microscopy images depict the localization of YFP alone under control of the 35S promoter or *Cauliflower mosaic virus* (35S::*YFP*; first column), *MAR1* chloroplast transit peptide fused to YFP (35S::*MAR1tp-YFP*; second column), full-length *MAR1* cDNA with YFP at the C terminus (35S::*MAR1-YFP*; third column), full-length *MAR1* cDNA with YFP at the N terminus (35S::*YFP-MAR1*; fourth column), and an untransformed protoplast (fifth column). A bright-field image (A, E, I, M, and Q), chlorophyll autofluorescence (B, F, J, N, and R), YFP fluorescence (C, G, K, O, and S), and a merge of the two channels (D, H, L, and P) are included for each protoplast. We note that T is a merge of all three channels (transmitted, chlorophyll, and YFP).

In short-term uptake experiments with isolated chloroplasts, it was found that chloroplasts from *mar1-1* mutant plants accumulated less gentamicin than wild-type (Landsberg *erecta* [L*er*]) controls, while chloroplasts from *MAR1* overexpressors accumulated the most gentamicin (Fig. 7, A and C). This experiment was performed a total of three independent times with the same result. In uptake experiments using whole seedlings, it was found that chloroplasts from *mar1-1* and *mar1-3* mutant seedlings accumulated less gentamicin than the wild-type (Columbia-0 [Col-0]) control (Fig. 7D). Evidence from these experiments demonstrates the role of MAR1 as a chloroplast-associated transporter that is capable of importing aminoglycoside antibiotic.

MAR1 May Have a Role in Iron Homeostasis

It is unlikely that evolutionary pressures would have selected for a means of entry for toxic antibiotics into plant chloroplasts. Therefore, we propose that MAR1 has a more conventional role in the plant, and the transport of antibiotics is an opportunistic effect. The expression pattern of *MAR1* does not yield many clues as to its potential function. Promoter-reporter fusion experiments using *MAR1*::*GUS* transgenic plants demonstrated that *MAR1* is expressed throughout the plant body in young seedlings (Supplemental Fig. S5, A and B). In addition, *MAR1* appears to be fairly evenly expressed in most tissue types based on AtGenExpress data (Supplemental Fig. S5C). Given its sequence similarity to *ferroportin*, it is possible that *MAR1* could be involved in some aspect of iron transport. In an attempt to test this possibility, we expressed *MAR1* cDNA in the yeast double mutant *fet3fet4*, which is defective in low and high affinity iron uptake (Dix et al., 1994). We found that *MAR1* expressed in vector pVV214 was unable to complement *fet3fet4* on SD media ±5, 10, or 20 μM $FeCl_3$ (data not shown). This result is probably not surprising, given MAR1's localization to the yeast mitochondria (Fig. 6D).

A common symptom of iron deficiency in plants is chlorosis, since iron is essential for chlorophyll biosynthesis (Vert et al., 2002). Interestingly, we observed a visible and quantifiable phenotype of chlorosis in 35S::*MAR1* seedlings when grown for 2 weeks on plain Murashige and Skoog (MS) media (Fig. 8B) or MS media supplemented with 50 μM Fe-EDTA (Fig. 8A, first plate). Additionally, when 35S::*MAR1* plants were grown in soil, they appeared slightly more chlorotic than the wild type, both in leaves and stems. Chlorosis was especially prominent along the midvein and older areas of cauline leaves, which also displayed an altered leaf shape, pinched toward the tip, compared to L*er* (Fig. 8D). Chlorosis of plate-grown seedlings persisted until media was supplemented with 300 μM Fe-EDTA (Fig. 8, A and C). Our results suggest that the overexpression of *MAR1* creates an iron-limiting condition for the plant.

One of the *MAR1* homologs in Arabidopsis, *AtIREG2*, was found to be up-regulated under iron deficiency (Schaaf et al., 2006). With this in mind, we examined *MAR1* for transcriptional changes under iron limita-

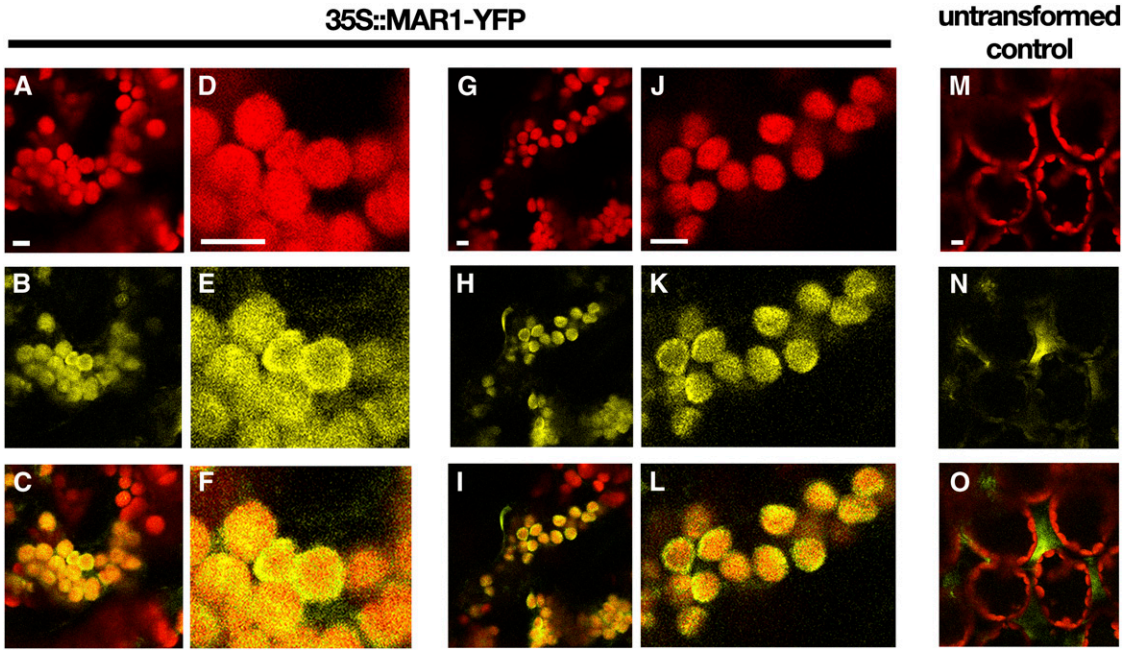

Figure 5. MAR1-YFP localizes to chloroplasts in leaves of transformed plants. Plants were transformed with the C-terminal fusion construct 35S::*MAR1-YFP* as described in "Materials and Methods." Confocal single-slice images of the leaves of two individually transformed plants (A–F and G–L) were compared to an untransformed leaf (M–O). D to F and J to L are close-up images of A to C and G to I, respectively. Chlorophyll autofluorescence (A, D, G, J, and M), YFP fluorescence (B, E, H, K, and N), and a merge of the two channels (C, F, I, L, and O) are shown for each leaf section. Bars = 8 μm.

tion and iron excess. Plants were grown in liquid culture for 14 d, and baseline tissue samples were taken before addition of either 600 μM Fe-EDTA (iron excess) or 300 μM ferrozine (iron limitation). We observed a 60% decrease in *MAR1* expression after 4 d of growth under iron deficiency (Fig. 9A), along with the expected up-regulation of *Iron Regulated Transporter1* (*IRT1*; which encodes for a major high-affinity iron transporter) under similar conditions (Stacey et al., 2008). We also observed a down-regulation of *MAR1* when plants were grown for 2 weeks on plates containing a lower concentration of ferrozine (100 μM; Fig. 9B). A subsequent increase in *MAR1* transcription was not observed when iron levels were elevated for 4 d (Fig. 9C), despite the expected down-regulation of *IRT1* under these conditions (Fig. 9C). Because the chlorosis of 35S::*MAR1* can be rescued by excess iron, and *MAR1* is down-regulated under limiting iron conditions, we postulate that *MAR1* may play a role in iron chelation, storage, or sequestration.

DISCUSSION

We have uncovered a mutant, *mar1-1*, which was found to be resistant to multiple aminoglycoside antibiotics (Fig. 1, A and B) based on a single point mutation in a putative transporter gene (Fig. 2, A and B). The resistance of *mar1-1* is highly specific for aminoglycosides that target prokaryotic translational machinery and does not extend even to the structurally similar aminocyclitol, spectinomycin (Fig. 1D). Thus, MAR1 is an example of a transporter capable of recognizing a very specific group of drugs.

The change of Ala to Val in the mar1-1 protein, given its location in the middle of a predicted transmembrane domain and the residue's high level of conservation among homologs in Arabidopsis and other plants (Fig. 2C), is likely to be very important to the function of MAR1. Additionally, MAR1 homologs that do not have Ala at position 441 replace this residue with either Ser or Gly (Fig. 2C), two amino acids with small R-groups. It is therefore likely that the addition of two relatively bulky methyl groups at this position in the mar1-1 mutant protein is enough to substantially alter MAR1 function. The nearly identical phenotypes of *mar1-1*, *mar1-2*, and *mar1-3* (Fig. 1, A and C) indicate that all alleles are probably hypomorphic mutations, and since all confer multiple resistance, the MAR1 transporter must be a means of entry for antibiotics. We confirmed this hypothesis by overexpressing *MAR1* in both wild-type and *mar1-1* backgrounds, which conferred hypersensitivity to multiple antibiotics (Fig. 3).

Since G418 and hygromycin do not cause chlorosis in plants, we were not able to do chlorophyll assays to determine resistance/sensitivity. However, we tested a wide range of concentrations and examined seedlings closely for phenotypic differences. We saw no difference in growth between *mar1-1* and wild-type L*er* at

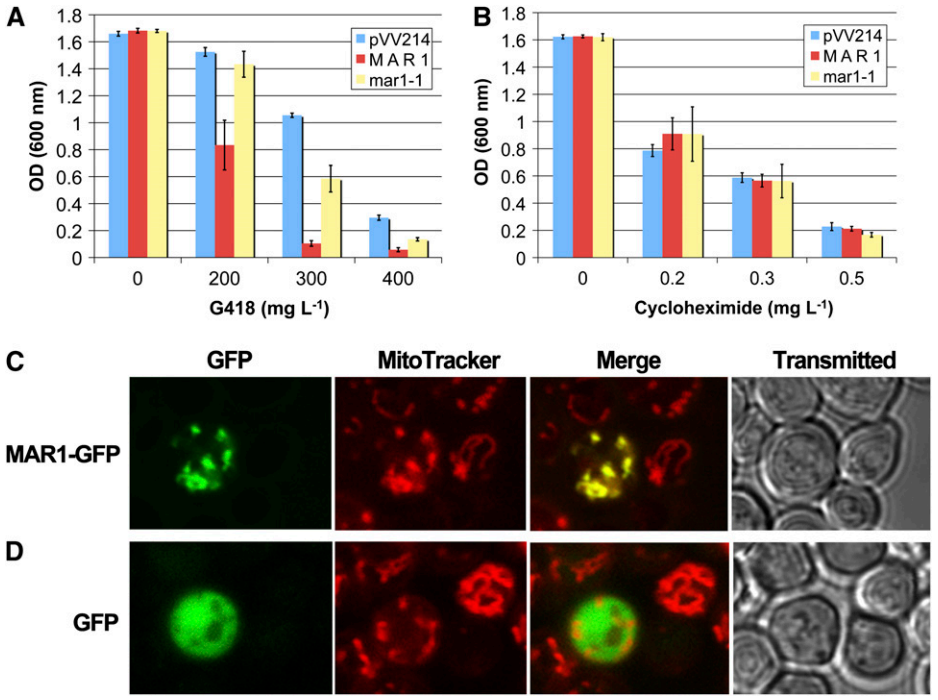

Figure 6. Expression of *MAR1* in yeast confers hypersensitivity to G418. A and B, *MAR1* and *mar1-1* were expressed in yeast under control of the PGK promoter (vector pVV214). Cultures were standardized to optical density (OD) 0.01 at 600 nm before addition of antibiotic (A, G418 at 0, 200, 300, and 400 mg/L; B, cycloheximide at 0, 0.2, 0.3, and 0.5 mg/L). Cultures were analyzed spectrophotometrically after 48 h of growth, and optical densities were plotted. For both graphs, each bar represents the average absorbance of three independent cultures (±SD). C and D, Yeast strain BY4700 was transformed using *MAR1* cDNA (lacking a stop codon) fused in frame with enhanced GFP (C) or using enhanced GFP alone (D). MitoTracker Red was used to visualize mitochondria, and a transmitted image is included to illustrate integrity of the cells.

any concentration (representative images are shown in Supplemental Fig. S1). Additionally, *mar1-1* was not resistant to the aminoglycoside paromomycin and appeared just as sensitized as the wild-type Col-0 (Supplemental Fig. S2), while plants expressing NPTII do show significant resistance (Supplemental Fig. S2, bottom row).

Since *mar1* mutants are sensitive to those particular aminoglycoside antibiotics that act in the cell cytoplasm (hygromycin, G418, and paromomycin; Supplemental Figs. S1 and S2) but resistant to those that act only in the chloroplast (kanamycin, tobramycin, gentamicin, streptomycin, amikacin, and apramycin; Fig. 1A), we would predict that these mutations act to keep antibiotics out of the chloroplast. In support of this hypothesis, we have successfully demonstrated that MAR1-YFP fusions localize to the chloroplast in both protoplasts (Fig. 4) and whole plants (Fig. 5). Additionally, we have shown that the MAR1 transit peptide coupled to YFP delivers the fluorophore to the chloroplast stroma (Fig. 4, F–H), while the addition of YFP at the N terminus blocks proper localization of the transporter (Fig. 4, N–P). Since the transit peptide is the site of specific interactions with TIC (for Translocon at the Inner envelope membrane of Chloroplasts) and TOC (for Translocon at the Outer envelope membrane of Chloroplasts) complexes of the chloroplast envelope, it is likely that the addition of a bulky YFP fluorophore ahead of this domain may interfere with these interactions, which are necessary for import (Dixit et al., 2006; Inaba and Schnell, 2008). Although we have yet to experimentally confirm whether MAR1 localizes to the inner or outer membrane of the chloroplast, the presence of an N-terminal transit peptide indicates that MAR1 is likely to localize specifically to the inner envelope, since most plastid proteins of the outer envelope do not possess these transit peptides (Hofmann and Theg, 2005; Jarvis, 2008).

In the yeast strain BY4700, it was found that MAR1 localized to the mitochondria (Fig. 6C), and its expression caused a strong increase in sensitivity to G418 (Fig. 6A). The mutant allele *mar1-1* also conferred sensitivity, albeit to a lesser extent. We hypothesize that the A-to-V mutation in mar1-1 causes a structural change in the transporter, such that its function is reduced. This reduced ability to function could be due to many factors, including reduced ability of the mutant transporter to bind or release substrate or reduced ability to bind or release a cotransported ion (such as Na^+ or H^+) used as an energy source for transport. Future experiments will enable us to distinguish between these and other possibilities.

To test the import function of MAR1 in a plant system, we performed uptake experiments using both isolated chloroplasts (Fig. 7A) and whole seedlings (Fig. 7D). To date, there is no report on uptake studies of aminoglycoside antibiotics in a plant system; therefore, no convenient assay was available. The assay developed here allows for inexpensive, nonradioactive detection of antibiotic and is based on the ability of aminoglycosides to adsorb onto nitrocellulose membrane without the need for fixation (Mihelic-Rapp and Giebel, 1996). Differences are clearly seen in lysate spots from *mar1-1* mutant chloroplasts, as compared to wild-type chloroplasts and chloroplasts from an overexpression line (Fig. 7C). These experiments provide evidence for the function of MAR1 as a transport protein.

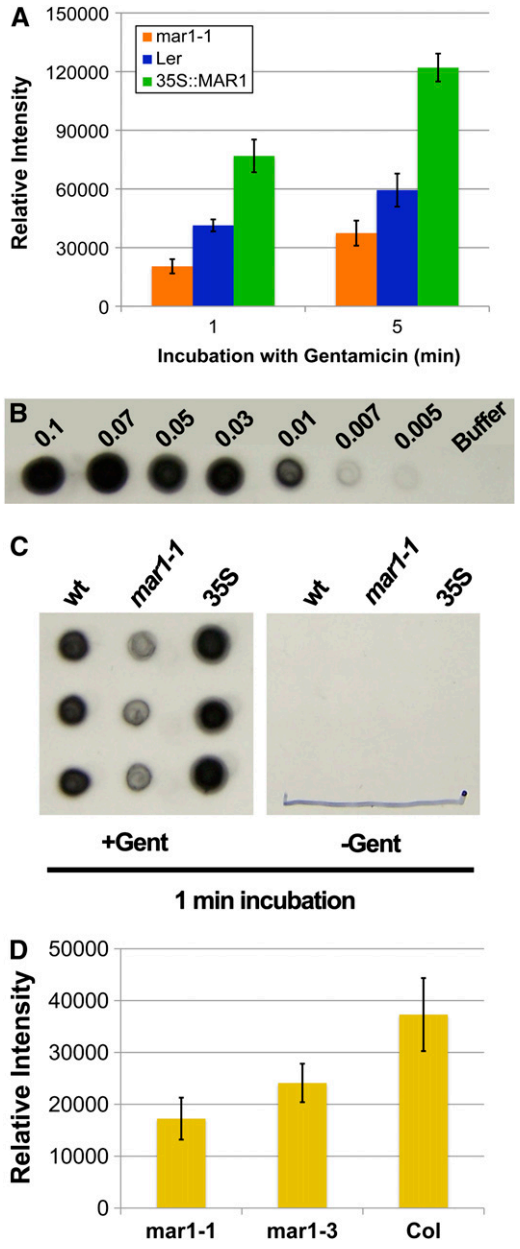

Figure 7. MAR1 regulates gentamicin entry into chloroplasts. A, Plants were grown for 15 d before chloroplast isolation, and 8.5×10^7 chloroplasts were incubated in 12.5 mg/mL gentamicin for each uptake reaction (1 and 5 min). B, Gentamicin standards (dissolved in chloroplast lysis buffer) were spotted as positive controls for every dot blot. Numbers above each dot indicate gentamicin concentration in mg/mL. C, Representative data from a 1-min uptake experiment. Left: Triplicate lysate spots from chloroplasts incubated with 12.5 mg/mL gentamicin for 1 min (+Gent). Right: Triplicate lysate spots from chloroplasts incubated in uptake buffer alone for 1 min (−Gent). In each panel, the left-hand column shows lysate from wild-type L*er* chloroplasts (wt), the middle column shows lysate from *mar1-1*, and the right-hand column shows lysate from 35S::*MAR1* overexpressor chloroplasts (35S). D, Whole seedling uptake results. Seedlings were exposed to 70 mg/L gentamicin for 2 d, washed, and chloroplasts isolated. Chloroplasts (3×10^8) from each line were lysed. For A and D, each bar represents the average relative intensity of three triplicate spots (±SD). [See online article for color version of this figure.]

A recent article describes independent mutations of the *MAR1* locus (At5g26820) that are sufficient to achieve kanamycin resistance in Arabidopsis (Aufsatz et al., 2009). These findings agree with our data; however, Aufsatz et al. report that resistance is kanamycin specific and does not carry over to gentamicin or hygromycin. We did not see hygromycin resistance in any of our *mar1* mutants, which was expected because hygromycin has effects against eukaryotic ribosomes and therefore acts in the cytoplasm of the plant cell (Eustice and Wilhelm, 1984). However, we do show that *mar1* mutants are multiply resistant to several aminoglycosides, including gentamicin (Fig. 1A). A possible reason for this discrepancy could be that the Aufsatz et al. mutations are distinct from our *MAR1* mutations (Fig. 2, A and B) and thus may confer slightly different phenotypes. We also note that Aufsatz et al. tested for gentamicin resistance at a concentration of 100 mg/L, while we test at 70 mg/L. Furthermore, Aufsatz et al. only mentioned the testing of kanamycin, hygromycin, and gentamicin—resistance to other aminoglycosides is not discussed.

The chlorosis phenotype of the *MAR1* overexpression line gives insight into the natural function of the MAR1 protein. Since this phenotype is rescued by iron feeding (Fig. 8, A and C), MAR1 may play a role in the chelation, storage, and/or sequestration of iron. If so, we might expect a decrease of *MAR1* transcript under iron limiting conditions, which is what was observed (Fig. 9, A and B). Under limiting conditions, we also saw the expected increase in the transcript of the major root iron transporter *IRT1*, which is highly up-regulated under iron limitation to increase the supply of iron to the plant cell (Eide et al., 1996; Korshunova et al., 1999; Rogers et al., 2000; Connolly et al., 2002). This up-regulation leads to an increase in cytoplasmic iron, but due to the poor substrate specificity of *IRT1*, it also results in increasing cytoplasmic levels of other toxic divalent metal cations, such as nickel. One of the *MAR1* homologs in Arabidopsis, *AtIREG2*, is proposed to play a role in the vacuolar sequestration of excess nickel accumulated under iron-limiting conditions due to the action of *IRT1* (Schaaf et al., 2006). Schaaf et al. showed that *AtIREG2* was up-regulated under iron deficiency, in contrast to *MAR1*, which is down-regulated (Fig. 9, A and B). Thus, we suggest that MAR1 and AtIREG2 play distinct roles in the plant cell. Their expression patterns are quite different: *AtIREG2* is mainly expressed in the root (Schaaf et al., 2006), while *MAR1* is highly expressed in all tissues (Supplemental Fig. S4C). AtIREG2 localizes to the vacuole (Schaaf et al., 2006), while MAR1 localizes to the chloroplast (Fig. 4). Despite these differences, we hypothesize that MAR1 and AtIREG2 both act to transport metal: AtIREG2 transports nickel into the vacuole, while MAR1 may be transporting iron in the chloroplast.

AtIREG1 was postulated to be involved in vessel loading of iron (Curie and Briat, 2003), and its down-regulation in *DwMYB2* overexpressors (Chen et al.,

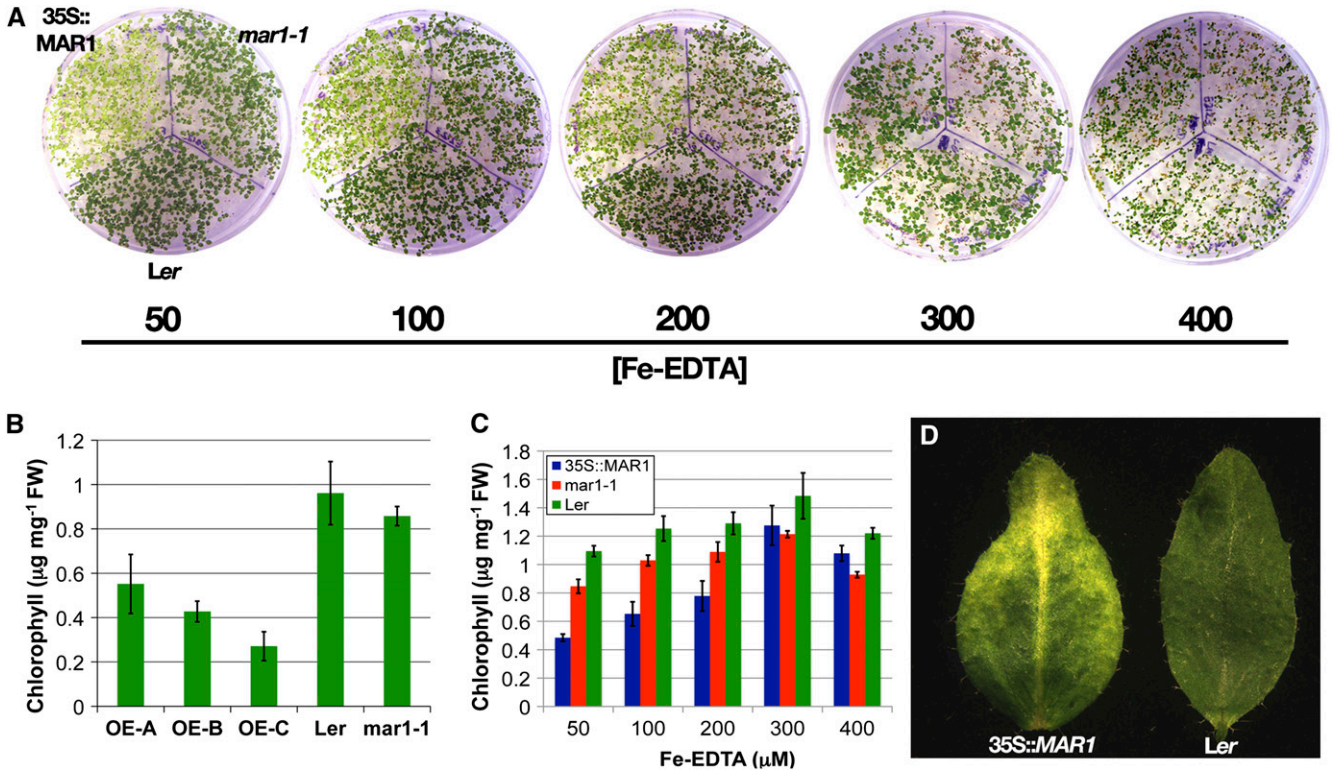

Figure 8. Chlorosis of 35S::*MAR1* is rescued by 300 μM Fe-EDTA. A, Plants were grown for 2 weeks on varying concentrations of Fe-EDTA (as indicated) before photographing. For each plate, the top left section contains 35S::*MAR1* seedlings, the top right contains *mar1-1* seedlings, and the bottom section contains L*er* wild-type seedlings. B, Chlorophyll content of three *MAR1* overexpression lines (OE-A, OE-B, and OE-C), L*er*, and *mar1-1* grown on MS plates supplemented with 1% Suc for 2 weeks (as described in "Materials and Methods"). C, Chlorophyll content of 35S::*MAR1*, *mar1-1*, and L*er* seedlings after 2 weeks growth on MS supplemented with varying concentrations of Fe-EDTA (as indicated). Chlorophyll was extracted and quantified as in B. FW, Fresh weight. D, Chlorosis phenotype of 35S::*MAR1* leaves from plants grown in soil for 32 d. [See online article for color version of this figure.]

2006) may be the cause of the disruption in iron translocation (from root to shoot) observed in these plants. Because citrate appears to be the major chelator for iron in the xylem (Haydon and Cobbett, 2007), it is possible that *AtIREG1* exports citrate (or an iron-citrate conjugate) from root cells into the vasculature, playing a role similar to *FRD3*, which mediates citrate efflux into root vasculature (Durrett et al., 2007). With this in mind, we postulate that MAR1 may also be acting to transport an iron chelator, such as citrate or nicotianamine (NA).

NA plays a key role in iron homeostasis by ensuring iron solubility in the weakly alkaline environment of the plant cytoplasm (Douchkov et al., 2005; Weber et al., 2008). Plants lacking NA (such as the tomato [*Solanum lycopersicum*] mutant *chloronerva*) show phenotypes of interveinal chlorosis in young tissues (Cassin et al., 2009). However, NA overaccumulation can paradoxically increase the sensitivity of Arabidopsis to iron deficiency by sequestering iron (Cassin et al., 2009). Since cytosolic iron homeostasis depends on NA (Hell and Stephan, 2003), and NA appears to be present in chloroplasts (Becker et al., 1995; Stephan, 1995), it may be possible that MAR1 transports NA into the chloroplast, where it likely is required to maintain iron solubility in the weakly alkaline environment of the stroma (Wu and Berkowitz, 1992).

The chlorosis phenotype of 35S::*MAR1* plants could be due to excess NA accumulating in the chloroplast, where it may sequester iron, creating the phenotype of iron deficiency. The phenotype observed in leaves of mature 35S::*MAR1* plants is the opposite of that seen in plants lacking NA (such as *chloronerva*); instead of interveinal chlorosis in young tissues, chlorosis arises in the midvein and in older tissues. This unusual chlorosis pattern may be the result of a redistribution of the cytoplasmic NA pool to the chloroplast. This has the dual effect of restricting NA from performing its role in phloem transport of iron and other metals (von Wiren et al., 1999) and also sequestering iron itself, thus preventing it from being redistributed throughout the plant body. Iron, applied in excess (300 μM), is able to rescue the chlorosis phenotype, and the *MAR1* gene is down-regulated under iron deficiency to prevent sequestration of needed iron. It may be that there is no increase in *MAR1* expression under iron excess

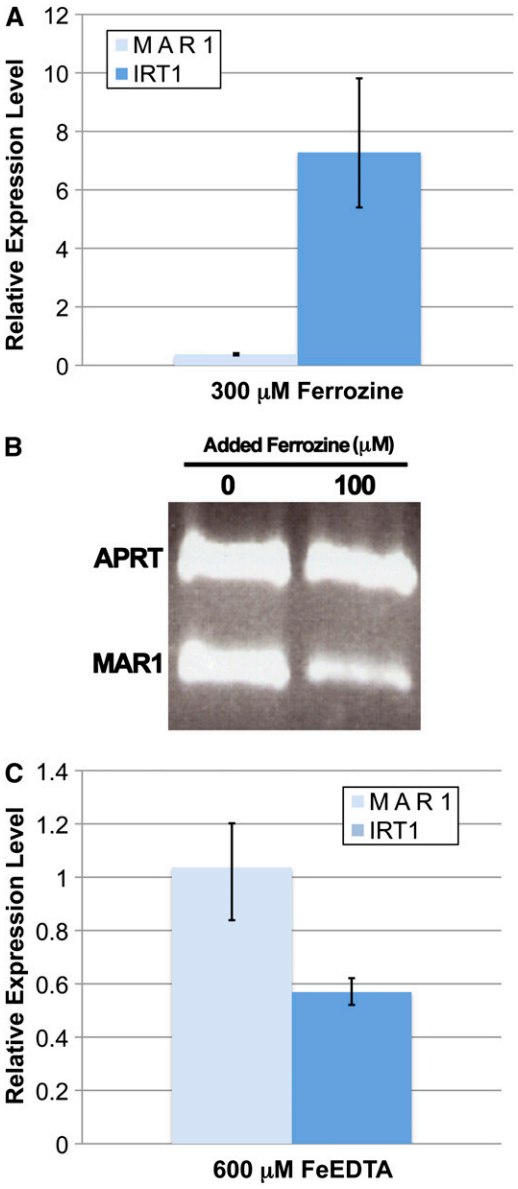

Figure 9. *MAR1* is down-regulated under iron deficiency. A, Plants were grown for 2 weeks in liquid MS supplemented with 1% Suc, and seedling tissue samples were taken before and after 4 d of incubation in 300 μM ferrozine. Expression levels of *IRT1* and *MAR1* are expressed as fold changes relative to their expression prior to ferrozine treatment. B, Plants were grown for 2 weeks on media containing 100 μM ferrozine prior to RNA extraction and reverse transcription-PCR. Equal amounts of each reaction were loaded on an agarose gel, and adenine phosphoribosyltransferase (APRT) was included as an internal control. C, Plants were grown exactly as in A, except that 600 μM Fe-EDTA was added on day 14 (instead of ferrozine). Expression levels of *IRT1* and *MAR1* are expressed as fold changes relative to their expression prior to Fe-EDTA treatment. [See online article for color version of this figure.]

(600 μM) due to the negative effects of NA overaccumulation (Cassin et al., 2009).

It is well known that aminoglycosides mimic polyamines and can use their inward transport systems for entering both bacteria and eukaryotic cells (Van Bambeke et al., 2000). Since NA is a polyamine (Ling et al., 1999), it may be a good potential candidate for a natural substrate of MAR1. This hypothesis will require further investigation. Since MAR1 is classified as a ferroportin, the possibility also remains that MAR1 is transporting iron, and the chlorosis seen in *MAR1* overexpressors is a result of oxidative damage caused by excess iron accumulation in the chloroplast. If this is the case, one possibility is that chlorosis of overexpressors is relieved in the presence of high levels of exogenous iron (300 μM) because at this level, the plant is likely to activate its many defense mechanisms against iron toxicity, such as down-regulation of *IRT1* and *AtNRAMP3* (Vert et al., 2002; Ravet et al., 2009), up-regulation of *AtFERRITIN1* (Gaymard et al., 1996), increasing NA production (Pich et al., 2001), and activation of responses against oxidative stress (Fourcroy et al., 2004). If *MAR1* does act to transport iron into the chloroplast, it may be regulated like *AtSBL*, a putative transporter hypothesized to import iron into chloroplasts for storage in ferritins (Wintz et al., 2003).

Both the chloroplast and mitochondria require metalloproteins for photosynthesis and respiration, respectively, though the question of how iron and other metals are allocated between the two organelles has not yet been addressed (Merchant et al., 2006). Since most photosynthetic components are down-regulated under iron limitation (Tognetti et al., 2007), one possibility is that under limiting conditions, iron is preferentially allocated to the mitochondria to maintain respiration. If this is the case, and MAR1 is acting to transport iron, we would expect to see a decrease in its expression under iron limitation, which is what was observed (Fig. 9, A and B).

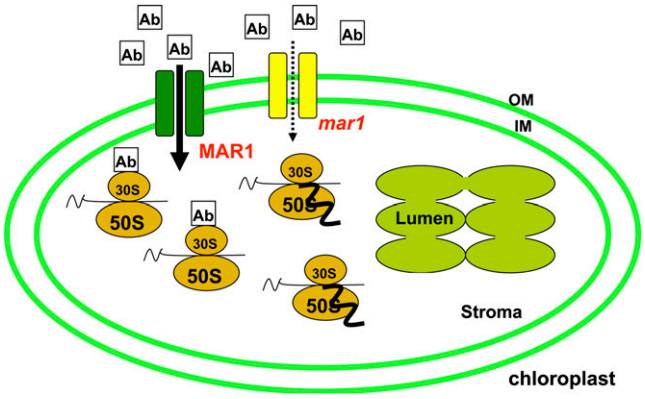

Figure 10. Model for function of MAR1. Aminoglycoside antibiotics enter the chloroplast through the MAR1 transporter to gain access to their ribosomal targets (aminoglycosides bind the 30S ribosomal subunit where they induce misreading and/or premature termination; Recht et al., 1999). The mutant *mar1-1* (indicated as *mar1*) is less functional, thus minimizing entry of antibiotics and conferring resistance. OM, Chloroplast outer membrane; IM, inner membrane; 30S, small ribosomal subunit; 50S, large ribosomal subunit; Ab, aminoglycoside antibiotic. [See online article for color version of this figure.]

mar1 represents an interesting example of plant antibiotic resistance that is based on the restriction of antibiotic entry into a subcellular compartment. Knowledge about this process, and other processes of antibiotic entry, could enable the production of crop plants that are incapable of antibiotic accumulation, aid in development of phytoremediation strategies for decontamination of water and soils polluted with antibiotics, and further the development of new plant-based molecular markers. This work also contributes to our understanding of how plants interact with the antibiotics they encounter, both in the laboratory (where aminoglycosides such as kanamycin are used heavily to select for transgenics) and in the natural environment.

These data indicate that MAR1 is a transport protein likely to be located on the chloroplast envelope, which appears to be capable of subcellular transport of multiple aminoglycoside antibiotics (Fig. 10). MAR1 is highly specific for aminoglycosides that act on prokaryotic translational machinery, since *mar1* mutants are not resistant to antibiotics of other classes, including those that act specifically in the chloroplast (Ellis, 1970; Kasai et al., 2004). Based on lack of sequence similarity, *MAR1* does not appear to belong to the ATP-binding cassette class of transporters previously implicated in Arabidopsis single antibiotic resistance. Instead, MAR1 may be transporting iron or a molecule involved in iron homeostasis. MAR1 is not able to distinguish between this molecule and the aminoglycosides. Further investigation is necessary to uncover the native function(s) of MAR1 in plant growth and development.

MATERIALS AND METHODS

Plant Materials and Growth Conditions

The original antibiotic resistant mutant, line E2-123 (*mar1-1*), was generated via EMS mutagenesis of line E2-6 (L*er* background, antibiotic sensitive; Kilby et al., 1992). The E2-6 line contains a methylation-silenced *nptII* gene at an unknown location. The original mutagenesis and screen was performed to try to identify components of the DNA methylation pathway. However, the T-DNA containing the silenced *nptII* gene segregates away from the *MAR1* locus. The original E2-123 (*mar1-1*) line was outcrossed to wild-type L*er* one time, and one subsequent homozygous *mar1-1* F2 progeny, without any T-DNA (verified by Southern-blot and PCR analysis), was used as the parent in the experiments presented here.

Plants were grown either in a growth room at 21°C, ambient humidity, under constant fluorescent illumination or on Petri dishes in a Percival chamber under similar conditions.

Plant Transformation

All constructs to be used in plant transformation experiments were transferred to *Agrobacterium tumefaciens* GV3101 via electroporation. Arabidopsis (*Arabidopsis thaliana*) plants were transformed by *Agrobacterium*-mediated transformation using the floral dip method (Clough and Bent, 1998). Primary transformants were selected in soil or on MS plates using the herbicide Basta (1.5 μL/mL; AgrEVO). The progeny of at least three selfed, primary transformants were used for experiments.

Map-Based Cloning of *MAR1*

A total of 608 kanamycin-resistant F2 progeny from a cross of the *mar1-1* mutant (F2 minus T-DNA as described above) to Col-0 and the *mar1-1* and Col-0 parents were genotyped using microsatellite loci polymorphic between Col-0 and L*er*. Resistant seedlings were selected after 2 weeks of growth on MS media plus kanamycin (25 mg/L). Genotype data were analyzed using MetaPhor agarose gels (Cambrex) and by fragment analysis using the Applied Biosystems 3730 genetic analyzer and GeneMapper software. Additional details are available in Supplemental Materials and Methods S1.

Gene Cloning and Plasmid Construction

All cloning was done using the Gateway system (Invitrogen). All *attB*-tailed PCR products were initially cloned into pDONR222 using BP Clonase and sequence verified before subcloning into various plant and yeast expression vectors (using LR Clonase) mentioned below.

35S::*MAR1*

The *MAR1* locus (At5g26820) was amplified by PCR (TripleMaster PCR system; Eppendorf) from L*er* (wild-type) genomic DNA using *attB*-tailed gene specific primers (Supplemental Table S1). *MAR1* was then subcloned into the plant overexpression vector pB7WG2 (Karimi et al., 2002) for subsequent *Agrobacterium*-mediated transformation of Col-0, L*er*, and *mar1-1* plants. At least three independent Basta-resistant transformed lines were isolated for analysis for each vector-genotype combination.

35S::*MAR1-YFP* and 35S::*YFP-MAR1*

MAR1 cDNA in vector pENTR/SD-DTOPO was obtained from the Arabidopsis Biological Resource Center stock center through The Arabidopsis Information Resource (www.arabidopsis.org, clone name: U16896). *MAR1* cDNA was amplified by PCR from this vector using specific primers (Supplemental Table S1). *MAR1* cDNA lacking a stop codon was subcloned into vector pH7YWG2 (Karimi et al., 2005) in frame to *YFP* for subsequent expression in Arabidopsis Col-0 protoplasts and *mar1-2* plants. N-terminal fusions (35S::*YFP-MAR1*) were constructed exactly as above, except that *MAR1* cDNA was cloned into the vector pB7WGY2 (in frame with *YFP*) and the stop codon was retained.

35S::*MAR1tp-YFP*

The first 162 nucleotides of *MAR1* were amplified by PCR using specific primers (Supplemental Table S1). Vector pH7YWG2 (Karimi et al., 2005) was used for subsequent expression in Arabidopsis Col-0 protoplasts.

Arabidopsis Protoplast Transformation

Protoplasts were isolated from 20-d-old seedlings and transformed according to methods previously described (Weigel and Glazebrook, 2002). Constructs used for transformation included 35S::*MAR1-YFP*, 35S::*YFP-MAR1*, 35S::*MAR1tp-YFP* (all described above), and 35S::*YFP* (pCL-eYFP-FL; a gift from Enamul Huq). Transformed protoplasts were allowed to incubate overnight under continuous light at 22°C prior to confocal microscopy.

Confocal Microscopy Analysis of 35S::*MAR1-YFP*, 35S::*MAR1tp-YFP*, and 35S::*YFP*

A Leica SP2 AOBS confocal laser scanning microscope was used for visualizing fluorescence images from Arabidopsis protoplasts and leaves. Excitation was at 514 nm, and the emission signal was collected between 525 and 590 nm for YFP fluorescence and between 622 and 700 nm for chlorophyll autofluorescence. Untransformed protoplasts and leaves were also examined as controls.

T-DNA Knockout Lines *mar1-2* and *mar1-3*

T-DNA insertion alleles were identified from the Salk Institute Genomic Analysis Laboratory collection. *mar1-2* carries a T-DNA insertion in the 11th exon of At5g26820 (Salk_034189, position 9436545 on chromosome V). *mar1-3* carries a T-DNA insertion in the 9th exon of At5g26820 (Salk_009286, position 9436095 on chromosome V). Lines were confirmed homozygous by PCR and by segregation analysis on kanamycin.

Quantification of Antibiotic Resistance in Plants

Titrations of the antibiotics kanamycin, gentamicin, streptomycin, tobramycin, amikacin, and apramycin were established to determine the concentration at which the greatest difference in resistance could be observed between the wild type and mutant *mar1-1* when plated on MS media plus antibiotic. These concentrations were determined to be 25 mg/L kanamycin, 70 mg/L gentamicin, 75 mg/L streptomycin, 40 mg/L tobramycin, 100 mg/L amikacin, and 200 mg/L apramycin. Seeds of mutant lines *mar1-1* and *mar1-2* along with a corresponding wild-type line (Col × L*er*, F4) and an unrelated kanamycin-resistant T-DNA insertion line (Salk_030942, which interrupts *MYB5*) were surface sterilized and plated onto MS media and MS plus antibiotic. After 48 h of vernalization, plates were moved to a 22°C incubator under constant light conditions for 14 d.

Measurement of Seedling Chlorophyll Content

Chlorophyll was extracted and quantified in triplicate according to methods described previously (Porra et al., 1989).

Yeast Transformation

MAR1 and *mar1-1* cDNAs were cloned into vector pVV214 (Van Mullem et al., 2003) via the Gateway method, and the *Saccharomyces cerevisiae* strains BY4700 (MAT**a** ura3Δ0) and *fet3fet4* (DEY 1453; MATα trp1 ura3 Δfet3::LEU2 Δfet4::HIS3; Eide et al., 1996) were transformed with these constructs (or empty vectors) using standard methods (Elble, 1992). The *fet3fet4* strain was always maintained in dropout media containing 0.2 mM $FeCl_3$ prior to testing for complementation on media supplemented with 0 to 50 μM $FeCl_3$ or Fe-citrate.

Yeast Antibiotic Susceptibility Assays

Eight individual clones from each line (described above) were selected from −URA dropout plates and PCR checked for the presence of the transgene. BY4700 transformed with pVV214 alone served as a control. Of the positive clones, three were selected and grown overnight at 30°C in 5 mL of −URA liquid dropout media. Cultures were then standardized to 0.01 optical density (λ600) before addition of various concentrations of G418 or cycloheximide (Fig. 6). After 48 h of growth at 30°C, OD_{600} was recorded for each culture. The experiment was carried out in triplicate.

MAR1 Localization in Yeast

MAR1 cDNA (with stop codon removed) was cloned into vector pAG426GPD-ccdB-EGFP (Addgene plasmid 14204) via the Gateway method, and the yeast strain BY4700 was transformed as described above. pAG426GPD-ccdB-EGFP alone was used as a control. A mixed population of transformed and untransformed cells was incubated in a 500 nM solution of MitoTracker Red CMXRos (Invitrogen) for 20 min at room temperature. A Leica SP2 AOBS confocal laser scanning microscope was used for visualizing fluorescence images. Excitation was at 514 nm, and the emission signal was collected between 525 and 540 nm for GFP fluorescence and between 600 and 650 nm for MitoTracker Red.

Chloroplast Isolation and Antibiotic Uptake Assays

Intact chloroplasts were isolated basically according to previous methods (Weigel and Glazebrook, 2002), with several modifications (Aronsson and Jarvis, 2002) to ensure that chloroplasts were import competent (see Supplemental Materials and Methods S1). Chloroplasts were consistently determined to be >80% intact based on photoreduction of ferricyanide (Sigma Chloroplast Isolation Kit Technical Bulletin; Sigma-Aldrich).

Chloroplasts were counted using a hemocytometer, and a standard number was used for each reaction (Fig. 7 legend). The uptake reaction buffer was HMS (50 mM HEPES-KOH [pH 8], 3 mM $MgSO_4$, 0.3 M sorbitol; see Supplemental Materials and Methods S1) +10 mM carbonate +0.2% (w/v) BSA. Gentamicin was added to a final concentration of 12.5 mg/mL, and uptake reactions were carried out on a rotator in a Percival chamber under constant fluorescent illumination for given time periods (Fig. 7A). Negative controls were incubated in HMS uptake buffer without gentamicin. To stop the uptake reaction, tubes were spun at 1,000*g* for 2 min in a microcentrifuge, supernatant was decanted, and chloroplasts were washed with 500 μL HMS buffer. This was repeated for a total of three washes. Chloroplasts were then incubated in 150 μL CP lysis buffer (20 mM HEPES, pH 7.5, 5 mM KCl, 1.5 mM $MgCl_2$, 10 mM dithiothreitol, 10% [v/v] glycerol, and 1% [w/v] polyvinylpyrrolidone) on ice for 1 h with occasional vortex. Supernatants were collected after centrifugation (3,000*g* for 5 min) and stored at −20°C until use in dot blot.

Dot blots for antibiotic detection in chloroplast lysates were performed as follows: 2 μL of each lysate was spotted onto nitrocellulose membrane (pore size 0.2 μM) in triplicate (Fig. 7C), along with 2 μL of each of a set of standard gentamicin solutions (in CP lysis buffer) as positive controls (Fig. 6B). Spotted membranes were allowed to dry for 45 min before blocking with 1× phosphate-buffered saline (PBS), pH 7.4, + 0.05% (v/v) Tween 20 + 5% (w/v) nonfat dry milk. Blocking time was 1 h on a rotary shaker at room temperature. After the block, mouse anti-gentamicin antibody (AbCam) was applied (in blocking solution) at 1:1,000 dilution, and incubation was carried out at 4°C overnight. The membrane was then washed two times for 15 min each with PBS, three times for 15 min each with PBS + 0.05% (v/v) Tween 20, and one time for 15 min with PBS.

Goat anti-mouse horseradish peroxidase-conjugated secondary antibody (Santa Cruz Biotechnology) was applied (in blocking solution) at a dilution of 1:5,000 and allowed to incubate for 1.5 h on a rotary shaker at room temperature. The above washes were then repeated. The membrane was allowed to incubate for 1 min in western Lighting Plus-ECL solution (Perkin-Elmer) before exposure to film (Kodak BIOMAX Light) for 10 s to 1 min. Images of developed film were analyzed using ImageJ64 (NIH). The image was inverted, and background was subtracted using a rolling ball radius between 60 to 80 pixels, depending on the blot (rolling ball radius should be equivalent to the size of the largest dot on the blot). The integrated density function was then used to measure the intensity of each dot. The average of three replicate dots (±SD) was graphed (Fig. 7A).

Whole Seedling Uptake

Approximately 2,000 seeds were sterilized for each line and vernalized for 2 d at 4°C in 100 mL volumes of liquid MS growth media. Flasks were then moved to a shaker in a Percival chamber (22°C, continuous fluorescent light). On day 11, the media were changed to fresh liquid MS. On day 13, gentamicin was added to a final concentration of 70 mg/L. On day 15, media were decanted and seedlings were washed with 300 mL of double distilled water. Chloroplasts were isolated from seedlings exactly as described above, and 3×10^8 chloroplasts from each line were lysed. The lysis protocol was the same as above, and dot blots were also performed as above, except that lysates were diluted 1:30 before spotting.

Gene Expression Analysis

Seeds from L*er* (wild type) were grown in Erlenmeyer flasks containing 200 mL liquid MS media supplemented with 1% Suc at 21°C under continuous white light on a shaker set to constant rpm in a Percival growth chamber. After 14 d of growth, several whole seedlings (roots and shoots) were removed, and RNA was extracted using the QIAgen RNeasy plant mini kit with on-column DNase treatment. Media were then supplemented with either 600 μM Fe-EDTA (iron excess) or 300 μM ferrozine (iron restriction), and remaining seedlings were allowed to incubate for a further 4 d. On day 4, RNA was extracted from remaining whole seedlings as above.

RNA (4 μg) from each sample was used in 40-μL reverse transcription reactions containing 250 nM *actin*, *IRT1*, and *MAR1* gene-specific reverse primers. For each target (*actin*, *IRT1*, and *MAR1*), five PCR reactions containing 400 nM primers and 2 μL of first-strand cDNA as a template were performed using SYBR green master mix (Applied Biosystems) and a spectrofluorometric thermal cycler (Applied Biosystems 7900HT). The comparative cycle threshold method was used to analyze the results (User Bulletin 2; Applied Biosystems PRISM sequence detection system).

For gel-based reverse transcription-PCR, plants were grown for 2 weeks on plates containing 0 or 100 μM ferrozine. On day 14, whole seedling tissue (root and shoot) was harvested and RNA extracted as above. Two micrograms of RNA was used as a template for each cDNA reaction (containing both *MAR1* and *APRT* primers), and equal amounts of cDNA reactions were loaded on a gel. Products were visualized with UV and ethidium bromide.

Sequence data for *MAR1* can be found in the GenBank data library under accession number At5g26820.

Supplemental Data

The following materials are available in the online version of this article.

Supplemental Figure S1. *mar1-1* is not resistant to the aminoglycosides hygromycin and G418.

Supplemental Figure S2. *mar1-1* is not resistant to the aminoglycoside paromomycin.

Supplemental Figure S3. Levels of *MAR1* expression in T-DNA lines (*mar1-2* and *mar1-3*) and 35S::*MAR1* overexpression lines (F2D and F2Y).

Supplemental Figure S4. Expression of *MAR1* in yeast does not affect sensitivity to chloramphenicol.

Supplemental Figure S5. *MAR1* expression pattern.

Supplemental Table S1. Primer sequences.

Supplemental Materials and Methods S1. Additional materials and methods.

ACKNOWLEDGMENTS

We thank Enamul Huq and Greg Hatlestad for helpful discussions and for critically reading the manuscript, David Eide for providing *fet3fet4*, Antonio Gonzalez for assistance with protoplast isolation protocols, Angela Bardo for help with confocal microscopy, and Enamul Huq for providing pCL-eYFP-FL.

Received June 26, 2009; accepted August 7, 2009; published August 12, 2009.

LITERATURE CITED

Aronsson H, Jarvis P (2002) A simple method for isolating import-competent Arabidopsis chloroplasts. FEBS Lett **529:** 215–220

Aufsatz W, Nehlin L, Voronin V, Schmidt A, Matzke A, Matzke M (2009) A novel strategy for obtaining kanamycin resistance in *Arabidopsis thaliana* by silencing an endogenous gene encoding a putative chloroplast transporter. Biotechnol J **4:** 224–229

Becker R, Fritz E, Manteuffel R (1995) Subcellular localization and characterization of excessive iron in the nicotianamine-less tomato mutant chloronerva. Plant Physiol **108:** 269–275

Boxall A, Johnson P, Smith E, Sinclair C, Stutt E, Levy L (2006) Uptake of veterinary medicines from soils into plants. J Agric Food Chem **54:** 2288–2297

Cassin G, Mari S, Curie C, Briat J, Czernic P (2009) Increased sensitivity to iron deficiency in *Arabidopsis thaliana* overaccumulating nicotianamine. J Exp Bot **60:** 1249–1259

Chander Y, Kumar K, Goyal S, Gupta S (2005) Antibacterial activity of soil-bound antibiotics. J Environ Qual **34:** 1952–1957

Chen Y, Wu X, Ling H, Yang W (2006) Transgenic expression of DwMYB2 impairs iron transport from root to shoot in *Arabidopsis thaliana*. Cell Res **16:** 830–840

Clough S, Bent A (1998) Floral dip: a simplified method for Agrobacterium-mediated transformation of *Arabidopsis thaliana*. Plant J **16:** 735–743

Connolly E, Fett J, Guerinot M (2002) Expression of the IRT1 metal transporter is controlled by metals at the levels of transcript and protein accumulation. Plant Cell **14:** 1347–1357

Curie C, Briat J (2003) Iron transport and signaling in plants. Annu Rev Plant Biol **54:** 183–206

Dix D, Bridgham J, Broderius M, Byersdorfer C, Eide D (1994) The FET4 gene encodes the low affinity Fe(II) transport protein of *Saccharomyces cerevisiae*. J Biol Chem **269:** 26092–26099

Dixit R, Cyr R, Gilroy S (2006) Using intrinsically fluorescent proteins for plant cell imaging. Plant J **45:** 599–615

Douchkov D, Gryczka C, Stephan U, Hell R, Baumlein H (2005) Ectopic expression of nicotianamine synthase genes results in improved iron accumulation and increased nickel tolerance in transgenic tobacco. Plant Cell Environ **28:** 365–374

Durrett T, Gassmann W, Rogers E (2007) The FRD3-mediated efflux of citrate into the root vasculature is necessary for efficient iron translocation. Plant Physiol **144:** 197–205

Eide D, Broderius M, Fett J, Guerinot M (1996) A novel iron-regulated metal transporter from plants identified by functional expression in yeast. Proc Natl Acad Sci USA **93:** 5624–5628

Elble R (1992) A simple and efficient procedure for transformation of yeasts. Biotechniques **13:** 18–20

Ellis R (1970) Further similarities between chloroplast and bacterial ribosomes. Planta **91:** 329–335

Emanuelsson O, Nielsen H, von Heijne G (1999) ChloroP, a neural network-based method for predicting chloroplast transit peptides and their cleavage sites. Protein Sci **8:** 978–984

Eustice D, Wilhelm J (1984) Mechanisms of action of aminoglycoside antibiotics in eucaryotic protein synthesis. Antimicrob Agents Chemother **26:** 53–60

Florini K, Denison R, Stiffler T, Fitzgerald T, Goldburg R (2005) Resistant Bugs and Antibiotic Drugs: State and County Estimates of Antibiotics in Agricultural Feed and Animal Waste. Environmental Defense, Washington, DC

Fourcroy P, Vansuyt G, Kushnir S, Inze D, Briat J (2004) Iron-regulated expression of a cytosolic ascorbate peroxidase encoded by the APX1 gene in Arabidopsis seedlings. Plant Physiol **134:** 605–613

Gaymard F, Boucherez J, Briat J (1996) Characterization of a ferritin mRNA from *Arabidopsis thaliana* accumulated in response to iron through an oxidative pathway independent of abscisic acid. Biochem J **318:** 67–73

Haydon M, Cobbett C (2007) Transporters of ligands for essential metal ions in plants. New Phytol **174:** 499–506

Hell R, Stephan U (2003) Iron uptake, trafficking and homeostasis in plants. Planta **216:** 541–551

Hocquet D, Vogne C, El Garch F, Vejux A, Gotoh N, Lee A, Lomovskaya O, Plesiat P (2003) MexXY-OprM efflux pump is necessary for adaptive resistance of *Pseudomonas aeruginosa* to aminoglycosides. Antimicrob Agents Chemother **47:** 1371–1375

Hofmann N, Theg S (2005) Chloroplast outer membrane protein targeting and insertion. Trends Plant Sci **10:** 450–457

Ibrahim N, Burke J, Beattie D (1974) The sensitivity of rat liver and yeast mitochondrial ribosomes to inhibitors of protein synthesis. J Biol Chem **249:** 6806–6811

Inaba T, Schnell D (2008) Protein trafficking to plastids: one theme, many variations. Biochem J **413:** 15–28

Jarvis P (2008) Targeting of nucleus-encoded proteins to chloroplasts in plants. New Phytol **179:** 257–285

Jeong J, Cohu C, Kerkeb L, Pilon M, Connolly E, Guerinot ML (2008) Chloroplast Fe(III) chelate reductase activity is essential for seedling viability under iron limiting conditions. Proc Natl Acad Sci USA **105:** 10619–10624

Karimi M, DeMeyer B, Hilson P (2005) Modular cloning and expression of tagged fluorescent protein in plant cells. Trends Plant Sci **10:** 103–105

Karimi M, Inze D, Depicker A (2002) Gateway vectors for Agrobacterium-mediated plant transformation. Trends Plant Sci **7:** 193–195

Kasai K, Kanno T, Endo Y, Wakasa K, Tozawa Y (2004) Guanosine tetra- and pentaphosphate synthase activity in chloroplasts of a higher plant: association with 70S ribosomes and inhibition by tetracycline. Nucleic Acids Res **32:** 5732–5741

Kavanagh TA, O'Driscoll KM, McCabe PF, Dix PJ (1994) Mutations conferring lincomycin, spectinomycin, and streptomycin resistance in *Solanum nigrum* are located in three different chloroplast genes. Mol Gen Genet **242:** 675–680

Kilby N, Leyser H, Furner I (1992) Promoter methylation and progressive transgene inactivation in Arabidopsis. Plant Mol Biol **20:** 103–112

Korshunova Y, Eide D, Clark W, Guerinot M, Pakrasi H (1999) The IRT1 protein from *Arabidopsis thaliana* is a metal transporter with a broad substrate range. Plant Mol Biol **40:** 37–44

Kumar K, Gupta S, Baidoo S, Chander Y, Rosen C (2005) Antibiotic uptake by plants from soil fertilized with animal manure. J Environ Qual **34:** 2082–2085

Larkin MA, Blackshields G, Brown NP, Chenna R, McGettigan PA, McWilliam H, Valentin F, Wallace IM, Wilm A, Lopez R, et al (2007) ClustalW and ClustalX version 2. Bioinformatics **23:** 2947–2948

Ling H, Koch G, Baumlein H, Ganal M (1999) Map-based cloning of chloronerva, a gene involved in iron uptake of higher plants encoding nicotianamine synthase. Proc Natl Acad Sci USA **96:** 7098–7103

Mackie R, Koike S, Krapac I, Chee-Sanford J, Maxwell S, Aminov R (2006) Tetracycline residues and tetracycline resistance genes in groundwater impacted by swine production facilities. Anim Biotechnol **17:** 157–176

Mellon M, Benbrook C, Benbrook K (2001) Hogging It: Estimates of Antimicrobial Abuse in Livestock. UCS Publications, Cambridge, MA

Mentewab A, Stewart CN Jr (2005) Overexpression of an *Arabidopsis thaliana* ABC transporter confers kanamycin resistance to transgenic plants. Nat Biotechnol **23:** 1177–1180

Merchant S, Allen M, Kropat J, Moseley J, Long J, Tottey S, Terauchi A (2006) Between a rock and a hard place: trace element nutrition in Chlamydomonas. Biochim Biophys Acta **1763:** 578–594

Mihelic-Rapp M, Giebel W (1996) A new immunohistochemical method for the detection of gentamicin in inner ear fluid compartments. Eur Arch Otorhinolaryngol **253:** 411–416

Paulsen I (2003) Multidrug efflux pumps and resistance: regulation and evolution. Curr Opin Microbiol **6:** 446–451

Pich A, Manteuffel R, Hillmer S, Scholz G, Schmidt W (2001) Fe homeostasis in plant cells: does nicotianamine play multiple roles in the regulation of cytoplasmic Fe concentration? Planta **213:** 967–976

Porra R, Thompson W, Kriedemann P (1989) Determination of accurate extinction coefficients and simultaneous equations for assaying chlorophyll a and chlorophyll b extracted with 4 different solvents - verification of the concentration of the chlorophyll standards by atomic-absorption spectroscopy. Biochim Biophys Acta **975:** 384–394

Ravet K, Touraine B, Boucherez J, Briat J, Gaymard F, Cellier F (2009) Ferritins control interaction between iron homeostasis and oxidative stress in Arabidopsis. Plant J **57:** 400–412

Recht M, Douthwaite S, Puglisi D (1999) Basis for prokaryotic specificity of action of aminoglycoside antibiotics. EMBO J **18:** 3133–3138

Rogers E, Eide D, Guerinot M (2000) Altered selectivity in an Arabidopsis metal transporter. Proc Natl Acad Sci USA **97:** 12356–12360

Rosellini D, LaFayette P, Barone P, Veronesi F, Parrott W (2004) Kanamycin-resistant alfalfa has a point mutation in the 16S plastid rRNA. Plant Cell Rep **22:** 774–779

Sarmah A, Meyer M, Boxall A (2006) A global perspective on the use, sales, exposure pathways, occurrence, fate and effects of veterinary antibiotics (VAs) in the environment. Chemosphere **65:** 725–759

Schaaf G, Honsbein A, Meda A, Kirchner S, Wipf D, von Wiren N (2006) AtIREG2 encodes a tonoplast transport protein involved in iron-dependent nickel detoxification in *Arabidopsis thaliana* roots. J Biol Chem **281:** 25532–25540

Scholar E, Pratt W (2000) The Antimicrobial Drugs, Ed 2. Oxford University Press, Oxford

Schwacke R, Fischer K, Ketelsen B, Krupinska K, Krause K (2007) Comparative survey of plastid and mitochondrial targeting properties of transcription factors in Arabidopsis and rice. Mol Genet Genomics **277:** 631–646

Schwacke R, Schneider A, Van Der Graaff E, Fischer K, Catoni E, Desimone M, Frommer W, Flugge U, Kunze R (2003) ARAMEMNON, a novel database for Arabidopsis integral membrane proteins. Plant Physiol **131:** 16–26

Stacey M, Patel A, McClain W, Mathieu M, Remley M, Rogers E, Gassmann W, Blevins D, Stacey G (2008) The Arabidopsis AtOPT3 protein functions in metal homeostasis and movement of iron to developing seeds. Plant Physiol **146:** 589–601

Stephan U (1995) The plant-endogenous Fe(II)-chelator nicotianamine restricts the ferrochelatase activity of tomato chloroplasts. J Exp Bot **46:** 531–537

Thomas C, Rajagopal A, Windsor B, Dudler R, Lloyd A, Roux S (2000) A role for ectophosphatase in xenobiotic resistance. Plant Cell **12:** 519–533

Tognetti V, Zurbriggen M, Morandi E, Fillat M, Valle E, Hajirezaei M, Carrillo N (2007) Enhanced plant tolerance to iron starvation by functional substitution of chloroplast ferredoxin with a bacterial flavodoxin. Proc Natl Acad Sci USA **104:** 11495–11500

Van Bambeke F, Balzi E, Tulkens P (2000) Antibiotic efflux pumps. Biochem Pharmacol **60:** 457–470

Van Mullem V, Wery M, DeBolle X, Vandenhaute J (2003) Construction of a set of *Saccharomyces cerevisiae* vectors designed for recombinational cloning. Yeast **20:** 739–740

Versaw W, Harrison M (2002) A chloroplast phosphate transporter, PHT2;1, influences allocation of phosphate within the plant and phosphate-starvation responses. Plant Cell **14:** 1751–1766

Vert G, Grotz N, Dedaldechamp F, Gaymard F, Guerinot M, Briat J, Curie C (2002) IRT1, an *Arabidopsis* transporter essential for iron uptake from the soil and for plant growth. Plant Cell **14:** 1223–1233

Vicens Q, Westhof E (2003) Crystal structure of geneticin bound to bacterial 16S ribosomal RNA A site oligonucleotide. J Mol Biol **326:** 1175–1188

von Wiren N, Sukhbinder K, Suhkibar B, Briat J, Khodr H, Shioiri T, Leigh R, Hider R (1999) Nicotianamine chelates both FeIII and FeII. Implications for metal transport in plants. Plant Physiol **119:** 1107–1114

Weber G, von Wiren N, Hayen H (2008) Investigation of ascorbate-mediated iron release from ferric phytosiderophores in the presence of nicotianamine. Biometals **21:** 503–513

Weigel D, Glazebrook J (2002) Arabidopsis: A Laboratory Manual. Cold Spring Harbor Laboratory Press, Cold Spring Harbor, NY

Windsor B, Roux SJ, Lloyd A (2003) Multiherbicide tolerance conferred by AtPgp1 and apyrase overexpression in *Arabidopsis thaliana*. Nat Biotechnol **21:** 428–433

Wintz H, Fox T, Wu Y, Feng V, Chen W, Chang H, Zhu T, Vulpe C (2003) Expression profiles of *Arabidopsis thaliana* in mineral deficiencies reveal novel transporters involved in metal homeostasis. J Biol Chem **278:** 47644–47653

Wu W, Berkowitz G (1992) Stromal pH and photosynthesis are affected by electroneutral K^+ and H^+ exchange through chloroplast envelope ion channels. Plant Physiol **98:** 666–672